The Magnetohydrodynamic Richtmyer-Meshkov Instability: The Transverse Field Case

V. Wheatley[1], R. Samtaney[2] and D. I. Pullin[3]

[1]School of Mechanical and Mining Engineering
University of Queensland, Queensland 4072, Australia

[2]Mechanical Engineering
King Abdullah University of Science and Technology, Thuwal 23955-6900, Saudi Arabia

[3]Graduate Aerospace Laboratories
California Institute of Technology, California 91125, USA

Abstract

The Richtmyer-Meshkov instability occurs when a perturbed interface between fluids of different densities is impulsively accelerated, typically by a shock wave. It is important in a number of applications including inertial confinement fusion, astrophysical phenomena and fuel-air mixing in scramjets. When the materials involved are in the plasma state, it has been shown that the instability can be suppressed by a magnetic field normal to the interface. The linearized case where the magnetic field is parallel to the interface has also been modelled analytically, but utilising a non-equilibrium initial condition. Here, we present an alternative model based on solving the linearized incompressible initial value problem with an equilibrium initial condition. This results in a simpler model for the interface behaviour that illustrates the effect of the impulsive acceleration only. The flow predicted by the incompressible model is compared to the results of two-dimensional, impulsively accelerated, compressible magnetohydrodynamic (MHD) simulations, which was not done previously for the parallel field case. The instability is found to also be suppressed in the parallel field case. The vortex sheet that is present on the interface immediately after the impulse breaks up into waves travelling parallel and anti-parallel to the magnetic field, which transport the vorticity. The interference of these waves, as they propagate, causes the perturbation amplitude of the interface to oscillate in time. This interface behaviour is accurately predicted by the linear model for the conditions investigated.

Introduction

When a shock wave interacts with a perturbed interface separating fluids with different densities, the interface becomes unstable and the perturbations grow. This scenario was first considered by Markstein [1]. A rigorous theoretical and numerical analysis of the flow was later presented by Richtmyer [2], whose predictions were confirmed by the shock tube experiments of Meshkov [3]. This instability is therefore known as the Richtmyer-Meshkov instability (RMI). The canonical situation in which the RMI occurs is shown in Figure 1(a), where a shock wave interacts with a sinusoidal density interface. Figure 1(b) shows the effect of the instability on the interface after the interaction is complete: it has become highly distorted which can lead to significant mixing between the two fluids.

The RMI is important in a wide variety of applications. One of the most significant of these is inertial confinement fusion (ICF), which has been a major impetus for the study of shock accelerated interfaces [4]. In current ICF experiments, rapid ablation of a spherical capsule of Beryllium-Copper alloy drives an implosion into the deuterium-tritium fuel contained within [5].
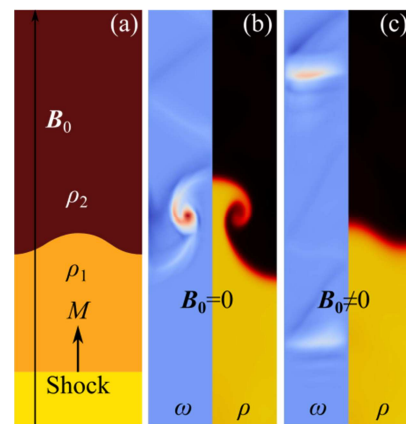

Figure 1. (a) Physical setup for the RMI simulations of Wheatley *et al*. [14]. Results shown are for an incident shock sonic Mach number of M=2, an initial magnetic field of non-dimensional strength $\beta^{-1} = B^2/2p_0 = 1/16$, where p_0 is the initial pressure, and a density ratio of ρ_2/ρ_1=1/3. (b) Post-interaction density (left half frame) and vorticity (ω, right half plane) fields when no magnetic field is present. (c) Post-interaction density and vorticity fields when a magnetic field is present.

The RMI promotes mixing between the capsule material and the fuel. This mixing limits the final compression of the fuel and hence the possibility of achieving energy break-even or production [6]. The RMI is also important in astrophysical phenomena. It has been used to account for the lack of stratification in the products of supernova 1987A and is required in stellar evolution models [7]. Other applications of the RMI include mixing enhancement in hypersonic air breathing engines [8], shock-flame interactions [9] and reflected shock-tunnels [10].

In the first two applications of the RMI listed above, inertial confinement fusion and astrophysical phenomena, the medium involved may be in the plasma state and hence be affected by magnetic fields. The effect of a magnetic field on the RMI had not been investigated until Samtaney [11] demonstrated, via numerical simulations, that for the magnetic field orientation shown in Figure 1(a) the growth of the RMI is suppressed. This can clearly be seen by comparing Figure 1(b), which shows the post-interaction density contours when no magnetic field is present, and Figure 1(c), which shows the result of an identical simulation carried out in the presence of a magnetic field. It was shown by Wheatley *et al*. [12] that the suppression of the instability is caused by changes in the shock refraction process at the interface with the application of a magnetic field that leave the interface vorticity free. Subsequently, Wheatley *et al*. [13] carried out an analytical linear analysis of an impulsively accelerated density interface in the presence of a normal

magnetic field. This successfully models the behaviour of the interface in the MHD RMI for weak shocks and magnetic fields [14]. The other canonical MHD RMI case, where the magnetic field is parallel to the density interface, was linearly modelled by Cao *et al.* [15]. However, their solution technique, which differs from that used in Wheatley *et al.* [13], results in oscillation of the interface even when no forcing is present. In addition, their model has not been compared to other results to assess its accuracy.

In the present work, we formulate a linear incompressible model for the MHD RMI when the magnetic field is parallel to the mean interface location, as shown in figure 2. The approach of Wheatley *et al.* [13] is used so that interface motion occurs only as a result of the impulsive acceleration and not due to the initial condition. The behaviour predicted by this model is then compared to the results of impulse driven simulations of the full nonlinear compressible ideal MHD equations. This allows both the appropriateness and accuracy of the model to be investigated and reveals new details of the flow physics.

Incompressible Model

The geometry of the problem under consideration is shown in figure 2 (a): A shock wave of sonic Mach number M impacts a sinusoidally perturbed density interface in the presence of a transverse magnetic field, $\boldsymbol{B}$. The corresponding incompressible model problem is shown in figure 2 (b). The shock acceleration is replaced by an impulsive acceleration in the z-direction, $V\delta(t)$, where $\delta(t)$ is the Dirac delta function in time and $V \ll c$, the speed of light. This accelerates uniform quiescent conducting fluids of densities ρ_1 and ρ_2, respectively, separated by an interface with initial perturbation amplitude η_0 and wavelength λ. The initial magnetic field, $\mathbf{B}_0 = B\hat{\mathbf{e}}_x$, is aligned with the mean interface location in the x-direction and has non-dimensional strength $\beta^{-1} = B^2/(2p_0)$, where p_0 is the uniform initial pressure.
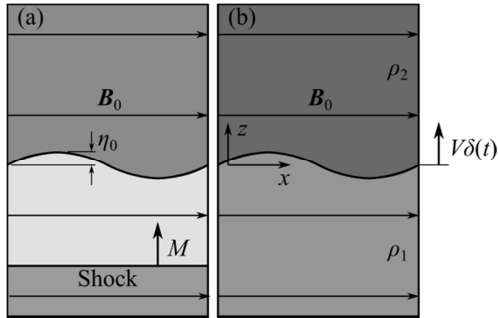
Figure 2. (a) Initial condition for compressible MHD RMI with transverse field. (b) Initial condition and geometry for corresponding incompressible model problem.

We seek solutions to this problem that satisfy the linearized equations of ideal, incompressible MHD. It is convenient to consider the situation where the fluid is restrained so that the impulsive body force $\rho V\delta(t)$ does not result in bulk motion of the fluid. The base-flow about which the equations are linearized results from subjecting uniform fluids separated by an unperturbed interface at $z = 0$ to the impulsive body force. The base-flow is independent of x and has zero horizontal velocity (u). An impulsive hydrostatic pressure distribution balances the body force resulting in the vertical velocity (w) also being zero. The complete base-flow is denoted with a subscript 0 and is given by

$\rho_0(z) = \rho_1 + H(z)(\rho_2 - \rho_1),$

$u_0 = 0, \; w_0 = 0, \; B_{x0} = B, \; B_{z0} = 0,$

$p_0(z,t) = -\rho_1 V\delta(t)z - H(z)(\rho_2 - \rho_1)V\delta(t)z,$

where $H(z)$ is the Heaviside function, ρ is density, p is pressure, $\mathbf{u}$ is velocity, and $\mathbf{B}$ is the magnetic field. The linearized equations for the perturbations to the base-flow are obtained by setting the density equal to

$\rho(\mathrm{x},z,t) = \rho_1 + H[z - h(x,t)](\rho_2 - \rho_1),$

where the interface location $h(x,t) \ll \lambda$, and by assuming that all other flow quantities have the form $q(x,z,t) = q_0(z) + q'(x,z,t)$, where q' are small perturbations to the base-flow. Substituting these expressions into the incompressible MHD equations and neglecting terms involving products of perturbations yields

$$\frac{\partial u\prime}{\partial x} + \frac{\partial w\prime}{\partial z} = 0, \tag{1}$$

$$\rho \frac{\partial u\prime}{\partial t} + \frac{\partial p\prime}{\partial x} = 0, \tag{2}$$

$$\rho \frac{\partial w\prime}{\partial t} + \frac{\partial p\prime}{\partial z} = (\rho_2 - \rho_1)[H(z) - H(z - h)]V\delta(t) - B\left(\frac{\partial B_{x\prime}}{\partial z} - \frac{\partial B_{z\prime}}{\partial x}\right), \tag{3}$$

$$\frac{\partial B_{x\prime}}{\partial x} + \frac{\partial B_{z\prime}}{\partial z} = 0, \tag{4}$$

$$\frac{\partial \mathbf{B}\prime}{\partial t} = B\frac{\partial \mathbf{u}\prime}{\partial x}. \tag{5}$$

The forcing of the perturbations due to the impulse at $t = 0^+$ is non-zero only in the vanishingly small region $z \in [0, h(x,t)]$. Our approach is to account for the forcing in the matching conditions between homogeneous solutions that are valid above and below this region. To obtain the homogenous solutions, we assume that all perturbations have the form $q'(x,z,t) = \hat{q}(z,t)e^{ikx}$ then take the temporal Laplace transforms of (1)-(5) outside of the forced region. Initial conditions are taken at $t = 0^-$, when there are no perturbations to the velocity or magnetic field. The transformed equations can then be combined to give a single differential equation for the transformed vertical velocity magnitude in each fluid,

$$D^2 W_j - k^2 W_j = 0, \tag{6}$$

where W is the temporal Laplace transform of $\hat{w}$, $j = 1$ or 2, s is the Laplace variable and $D \equiv \mathrm{d}/\mathrm{d}z$. Equations (6) has the general solution

$$W_j = A_j(\mathrm{s})e^{kz} + B_j(\mathrm{s})e^{-kz}. \tag{7}$$

This is relatively simpler than the general solution for the normal field case, which had additional terms corresponding to wave-like modes of the form $H(t \pm z\sqrt{\rho_j}/B_{\mathrm{z}})f(t \pm z\sqrt{\rho_j}/B_{\mathrm{z}})$ [13]. These modes were responsible for transporting the vorticity generated by impulse away from the interface, which suppressed its growth [14]. Thus the mechanism by which the RMI was suppressed in the normal field case is absent here.

As the perturbations must be bounded as $|z| \to \infty$, assuming $k > 0$, $A_2(s) = 0$ and $B_1(s) = 0$. Thus the transformed velocity magnitudes in each fluid are

$$W_1(z,s) = A_1(s)e^{kz}, \; W_2(z,s) = B_2(s)e^{-kz}. \tag{8}$$

These homogeneous solutions are subject to matching conditions at the contact ($z = h(x,t) = \eta(t)e^{ikx}$). Only two matching conditions are required to determine the solution in this case. The first is the kinematic condition that w' must be continuous. To leading order in h, this is equivalent to

$$[W]_{z=0} = 0 \to A_1(s) = B_2(s) \equiv A(s), \tag{9}$$

where $[q]_{z=0} \equiv q_2|_{z=0} - q_1|_{z=0}$ and (8) was used to obtain the expression on the right.

The second matching condition, which accounts for the forcing, is derived by integrating (3) in z across the inhomogeneous

region, from 0 to $h(x,t)$. After using the fact that $p + \frac{1}{2}\boldsymbol{B} \cdot \boldsymbol{B}$ is continuous across the contact, expanding quantities evaluated at $z = h$ as Taylor series about $z = 0$, and neglecting products of perturbations and higher order terms in h, this integration yields

$$p_2'(x,0,t) - p_1'(x,0,t) + B[B_{x2}'(x,0,t) - B_{x1}'(x,0,t)]$$
$$= (\rho_2 - \rho_1)V\delta(t)\eta(t)e^{ikx}. \qquad (10)$$

Equations (1)-(5) can be used to express p_j' and B_{xj}' in terms of w_j'. Using these expressions, taking the Laplace transform of (10) and using (8) gives

$$\left[(\rho_1 + \rho_2)\frac{s}{k} + \frac{2kB^2}{s}\right]A(s) = (\rho_2 - \rho_1)V\eta_0. \qquad (11)$$

The final solutions for the vertical velocity perturbations are obtained by solving for (10) for $A(s)$, taking the inverse Laplace transform, then substituting the result in the assumed forms of the perturbations. This gives

$$w_1'(x,z,t) = kV\eta_0\mathcal{A}\cos(\omega t)\,\mathrm{H}(t)e^{kz}e^{ikx}, \qquad (12)$$

$$w_2'(x,z,t) = kV\eta_0\mathcal{A}\cos(\omega t)\,\mathrm{H}(t)e^{-kz}e^{ikx}, \qquad (13)$$

where

$$\omega = \frac{Bk}{\sqrt{(\rho_1+\rho_2)/2}} = \frac{k}{\sqrt{\frac{1}{2}(c_{A1}^{-2}+c_{A2}^{-2})}}, \qquad \mathcal{A} \equiv \frac{\rho_2-\rho_1}{\rho_2+\rho_1}.$$

Here, $\mathcal{A}$ is the Atwood ratio and $c_{Aj} = B/\sqrt{\rho_j}$ is the Alfvén speed. This solution shows that while the initial ($t = 0^+$) growth rate of the interface,

$$\left.\frac{\partial\eta}{\partial t}\right|_{t=0} = w_j'(0,0,0^+) = \eta_0 kV\mathcal{A}, \qquad (14)$$

is identical to the hydrodynamic case [2], the presence of the magnetic field prevents linear growth at this rate. Instead, the amplitude of the interface oscillates in time at a frequency ω, as described by

$$\eta(t) = \int_{0^+}^t w_j'(0,0,\tau)d\tau = \eta_0\left(1 + \frac{kV\mathcal{A}}{\omega}\sin(\omega t)\right). \qquad (15)$$

For one set of parameters, the resulting density field at $t = 0.2\pi/\omega$ is shown in figure 3 along with the magnetic field lines. It can be seen that the motion of the interface has perturbed the magnetic field lines, which creates a restoring force due to magnetic field line tension. This causes the fluids to oscillate, but we will see that it does not completely describe the flow physics around the
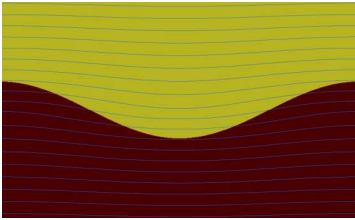

Figure 3. Density field and magnetic field lines from the incompressible linear MHD RMI model at $t = 0.2\pi/\omega$. Results shown are for the case with $\beta = 1, V = 2, \eta_0 = \lambda/20$ and $\rho_2/\rho_1 = 3$.

interface.

One aspect of the solution that requires further investigation is the nature of the interface. The unperturbed interface has no magnetic field lines crossing it and is what is known as a tangential discontinuity. Only the normal velocity w and $p + \boldsymbol{B} \cdot \boldsymbol{B}/2$ are required to be continuous across a tangential discontinuity (see e.g. [16]), and this is all we have assumed in our solution. If the field lines cross the interface, however, as is seen to occur in figure 2, two additional jump conditions must be

satisfied. These are the continuity of tangential velocity and magnetic field. From our solution, we find the jump in tangential velocity across the interface is non-zero and is given by

$$[u]_{z=0} = 2V\eta_0\mathcal{A}\cos(\omega t)\,\mathrm{H}(t)\sin(kx). \qquad (16)$$

This implies that the inhomogeneous region between the two fluids, which we integrated across in our solution, must contain more structure than a simple MHD contact discontinuity. Additional structures must be present in this matching region to carry the shear. To investigate the nature of these structures, and determine if our model that integrates across them accurately predicts the motion of the interface, we turn to non-linear compressible simulations.

Simulation Methodology

The non-linear simulations were carried out using a compressible ideal MHD code similar to that used in Samtaney [11,17]. It uses an eight-wave upwinding formulation within an unsplit upwinding method [18,17]. The solenoidal property of the magnetic field is enforced at each time step using a projection method [17].

Both impulse-driven and shock-driven simulations have been carried out. The geometry for these simulations is as shown in figure 2. Periodic boundary conditions are used in the x-direction and zero gradient boundary conditions are used in the z-direction. A uniform grid spacing of $\lambda/256$ is used for all simulations.

For the shock-driven simulation, the initial densities below and above the interface are $\rho_1 = 1$ and $\rho_2 = 1.25$, respectively. The shock has a sonic Mach number $M = 1.25$ and the pressure upstream of the shock is $p_0 = 1$. The initial perturbation amplitude of the interface is $\eta_0/\lambda = 0.05$ and the uniform horizontal magnetic field upstream of the shock is characterized by $\beta = 8$. The shock-interaction process compresses the fluids to higher densities and pressure, slightly increases the magnetic field strength and compresses the interface perturbation. Post-shock-compression values are used to initialize the impulse-driven simulation. These are $\rho_1 = 1.26$, $\rho_2 = 1.57$, $p_0 = 1.47$, $B_{x0} = 0.628$ and $\eta_0 = 0.0395\lambda$. The magnitude of the impulse is set to the velocity imparted to the interface in the shock driven problem; $V = 0.296$. In the impulse-driven simulation, the forcing on the right-hand-side of (3) is imposed as a source term.

Results and Discussion

The evolution of vorticity in the vicinity of the interface from the impulse-driven simulation is shown in figure 4. The plots have been rotated by $90°$ to allow the evolution to be displayed compactly. The vorticity distribution immediately after the impulse is coincident with the contact discontinuity and is identical to that in hydrodynamic (zero magnetic field) case, as predicted by the linear model. If the vorticity remained on the contact, as at $t = 0^+$, it would cause the perturbation of the interface to grow and eventually for roll-up to occur. This situation cannot persist, however, as the MHD Rankine-Hugoniot
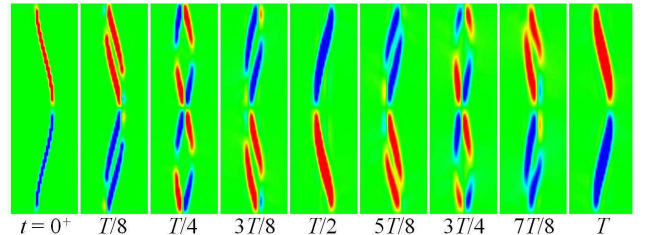

$t = 0^+ \quad T/8 \quad T/4 \quad 3T/8 \quad T/2 \quad 5T/8 \quad 3T/4 \quad 7T/8 \quad T$

Figure 4. Evolution of vorticity in the vicinity of the interface for an impulse-driven MHD RMI simulation with $\rho_1 = 1.26$, $\rho_2 = 1.57$, $p_0 = 1.47$, $(B_{x0}, B_{z0}) = (0.628, 0)$, $\eta_0 = 0.0395\lambda$ and $V = 0.296$. T is the model period $2\pi/\omega$. Red (blue) indicates positive (negative) vorticity.

relations prohibit steady shear across a contact discontinuity when magnetic field lines cross the discontinuity. Instead, we find that the initial distribution breaks up into two vorticity-carrying waves that propagate parallel and anti-parallel to the magnetic field at the relevant Alfén speed. In figure 4, it can be seen that the structure of these waves remains unchanged as they interact with each other. At $t = T/2$, where $T = 2\pi/\omega$ is the theoretical period from the linear model, the waves constructively interfere to form a vorticity distribution 180° out-of-phase with the original. This will reverse the growth of the interface perturbation caused by the vorticity distribution at $t = 0^+$. The periodic constructive interference of the waves continues indefinitely and causes the interface to oscillate in time. Similar waves were observed to occur in the shock driven case.

We have now established that waves do exist in the vicinity of the interface to support shear across the matching region while allowing the contact discontinuity to satisfy the relevant jump conditions. What remains to be investigated is whether our model, which integrates across this region, can accurately predict the behaviour of the interface. This is assessed in figure 5, which shows the interface amplitude histories from the incompressible model and both shock-driven and impulse-driven compressible simulations. It can be seen that the model accurately predicts both the oscillatory nature and frequency of the interface motion. The amplitude of the oscillations in the impulse driven simulation is almost perfectly predicted for the first half-period, but is somewhat under-predicted thereafter. The amplitude of the oscillations in the shock-driven simulation is smaller than in the corresponding impulse-driven simulation and is somewhat over-predicted by the model. We note that the interface oscillations in the shock-driven simulation deviate from sinusoidal behaviour in that the rate of decay of the perturbation amplitude is greater than the rate of growth.
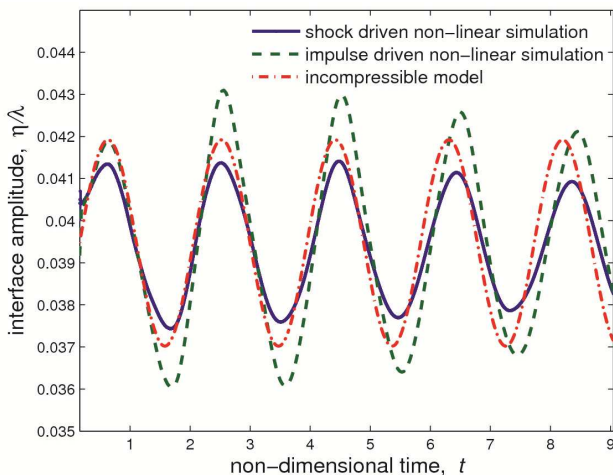

Figure 5. Interface amplitude histories from the linear incompressible MHD RMI model and non-linear simulations for the case corresponding to a shock-driven flow with $\rho_1 = 1$, $\rho_2 = 1.25$, $M = 1.25$, $p_0 = 1$, $\eta_0/\lambda = 0.05$ and a uniform horizontal magnetic field upstream of the shock characterized by $\beta = 8$.

Conclusions

We find that the MHD Richtmyer-Meshkov instability is suppressed in the transverse field case. The vortex sheet present on the interface immediately after the impulse breaks up into waves travelling parallel and anti-parallel to the magnetic field, which transport the vorticity. The interference of these waves as they propagate causes the perturbation amplitude of the interface to oscillate in time. This interface behaviour is accurately predicted by the incompressible linear model we have developed.

References

[1] G. H. Markstein. Flow disturbances induced near a slightly wavy contact surface, or flame front, traversed by a shock wave. *J. Aero. Sci.*, 24:238–239, 1957.

[2] R. D. Richtmyer. Taylor instability in shock acceleration of compressible fluids. *Comm. Pure and Appl. Math.*, 13:297–319, 1960.

[3] E. E. Meshkov. Instability of the interface of two gases accelerated by a shock wave. *Sov. Fluid Dyn.*, 4:101–108, 1969.

[4] M. Brouillette. The Richtmyer-Meshkov instability. *Ann. Rev. Fluid Mech.*, 34:445–468, 2002.

[5] J. D. Lindl, P. Amendt, R. L. Berger, S. G. Glendinning, S. H. Glenzer, S. W. Haan, R. L. Kauffman, O. L. Landen and L. J. Suter. The physics basis for ignition using indirect-drive targets on the National Ignition Facility. *Phys. Plasmas*, 11:339-479, 2004.

[6] J. D. Lindl, R. L. McCrory, and E. M. Campbell. Progress toward ignition and burn propagation in inertial confinement fusion. *Physics Today*, 45:32–40, 1992.

[7] D. Arnett. The role of mixing in astrophysics. *Ap. J. Suppl.*, 127:213–217, 2000.

[8] J. Yang, T. Kubota, and E. E. Zukoski. Applications of shock induced mixing to supersonic combustion. *AIAA J.*, 31:854–862, 1993.

[9] A. M. Khokhlov, E. S. Oran, and G. O. Thomas. Numerical simulation of deflagration to- detonation transition: the role of shock-flame interactions in turbulent flames. *Combust. Flames*, 117:323–339, 1999.

[10] R. J. Stalker and K. C. A. Crane. Driver gas contamination in a high-enthalpy reflected shock-tunnel. *AIAA J.*, 16:277–279, 1978.

[11] Ravi Samtaney. Suppression of the Richtmyer-Meshkov instability in the presence of a magnetic field. *Physics of Fluids*, 15(8):L53–L56, 2003.

[12] V. Wheatley, D. I. Pullin, and R. Samtaney. Regular shock refraction at an oblique planar density interface in manetohyrodynamics. *J. Fluid. Mech.*, 522:179, 2005.

[13] V. Wheatley, R. Samtaney, and D. I. Pullin. Stability of an impulsively accelerated perturbed density interface in incompressible MHD. *Phys. Rev. Letters,* 95, 2005.

[14] V. Wheatley, R. Samtaney, and D. I. Pullin. The Richtmyer–Meshkov instability in magnetohydrodynamics. *Phys. Fluids*, 21:082102, 2009.

[15] J. T. Cao, Z. W. Wu, H. J. Ren, and D. Li. Effects of shear flow and transverse magnetic field on Richtmyer-Meshkov instability. *Phys. Plasmas,* 15, 2008.

[16] G.W. Sutton and A. Sherman, *Engineering Magnetohydrodynamics*, McGraw-Hill, 1965.

[17] R. Samtaney, P. Colella, T. J. Ligocki, D. F. Martin, and S. C. Jardin, An adaptive mesh semi-implicit conservative unsplit method for resistive MHD, *Journal of Physics: Conference Series*, 16:40, 2005.

[18] P. Colella, Multidimensional upwind methods for hyperbolic conservation laws, *J. Comput. Phys.,* 87:171, 1990.